# *Macrophomina phaseolina*: Spatial Patterns in a Cultivated Soil and Sampling Strategies

J. D. Mihail and S. M. Alcorn

Department of Plant Pathology, University of Arizona, Tucson 85721.
Arizona Agricultural Experiment Station Journal Paper 4247.
This work was supported in part by USDA Grant 84-CSRS-2-2366.
The technical assistance of S. Gaul is gratefully acknowledged. The advice and assistance of T. Orum is appreciated.
Accepted for publication 13 January 1987 (submitted for electronic processing).

## ABSTRACT

Mihail, J. D., and Alcorn, S. M. 1987. *Macrophomina phaseolina:* Spatial patterns in a cultivated soil and sampling strategies. Phytopathology 77:1126-1131.

The spatial pattern of microsclerotia of *Macrophomina phaseolina* was determined from the assay of 2,250 soil samples taken from three blocks of 750 quadrats (1.0 × 0.3 m) in a cultivated field at Marana, AZ. This spatial pattern was aggregated as measured by the mean-to-variance ratio and Morisita's index of dispersion. Aggregate size was determined for each block using Morisita's index of clumping. Based on Moran's I, a statistic of spatial autocorrelation, significant positive autocorrelation was found among quadrats in all three blocks, indicating that similar levels of inoculum density tended to occur in quadrats of close proximity. Because the spatial pattern of microsclerotial population was found to be nonrandom, systematic sampling strategies were found to be most useful for mean estimation. Comparisons probabilistic and systematic sampling strategies are discussed.

*Additional key word*: charcoal rot.

Any collection of organisms has a spatial arrangement, that, when described, may help in the elucidation of the organism's ecology. Campbell and Noe (6) describe four major approaches to the characterization of spatial pattern based on quadrat count data. First, the populations may be mapped for easy visual interpretation of the data. Second, using goodness-of-fit techniques, discrete probability distributions may be fit to the data and conclusions drawn concerning the randomness or nonrandomness of the spatial pattern (7,11,15,18,24,28,29,36). Third, the degree of pattern departure from randomness may be measured by one of several indices of dispersion such as the variance-to-mean ratio or Morisita's index of dispersion (2,3,12,17,21,27,36). Fourth, techniques such as spectral analysis, lag analysis, and autocorrelation analysis may be used to more carefully characterize spatial patterns, by using the location of each quadrat (22,23,28,36).

Sampling soil for microorganisms has generally involved traversing one of several arbitrary paths (e.g., X, W, diagonal) through a field and collecting one or more samples at each of several sites along the path. An alternate approach involves the probabilistic selection of sampling sites using simple random sampling, stratified random sampling, cluster sampling, or other survey sampling techniques (26). Several studies have examined field sampling methodologies using both simulated and actual field data (14–16,24).

*Macrophomina phaseolina* (Tassi) Goid. is a soilborne fungus that causes charcoal rot of many crops in arid and semiarid areas of the world (10) and has been recovered from cultivated and noncultivated soils in Arizona (37,38). Several studies on the vertical pattern of microsclerotia of *M. phaseolina* in soil have demonstrated the highest concentration of inoculum in the top 30 cm (4,19). However, we are unaware of any published descriptions of the horizontal pattern of microsclerotia of *M. phaseolina* in soil. An understanding of the propagule spatial pattern of this soilborne phytopathogen would facilitate explanation and prediction of observed disease patterns. The objectives of the present study, therefore, were to characterize the spatial pattern of *M. phaseolina* in a cultivated soil and to evaluate sampling strategies to determine which would be most appropriate for the spatial pattern observed, given no a priori knowledge of that spatial pattern.



## MATERIALS AND METHODS

**Soil collection and processing.** In March 1985, soil samples were collected from a field, with Gila loam soil, located at the University of Arizona, Marana Agricultural Center. The field consisted of 15 contiguous beds, on 1.02-m centers and 48.77 m in length, subdivided into three 15.24- × 15.24-m blocks; 1.52 m separated each block. Each block was divided into 750 (1.02 × 0.3 m) nonoverlapping quadrats in a grid of 15 by 50 quadrats, for a total of 2,250 quadrats in the field. One 2.5- × 30-cm soil sample was taken from the center of each quadrat at a position corresponding to the precise location where guayule (*Parthenium argentatum* Gray) seedlings were later hand-transplanted. In addition, 10 soil cores were taken arbitrarily from the entire field and bulked ("bulk soil sample"). Each soil sample was air-dried, crushed through a 2-mm-mesh sieve, and mixed thoroughly. For each soil sample, one 3-g subsample was assayed for the microsclerotial population of *M. phaseolina* by using the semiselective medium and technique previously described (19). The use of a single subsample involved only a small sacrifice in accuracy (5), while allowing for the processing of a larger number of samples than would otherwise have been possible if repeated subsampling were necessary. At weekly intervals, throughout the processing of soil samples, one 3-g subsample from the bulk soil sample was assayed to monitor possible deterioration of microsclerotia of *M. phaseolina* in the soil samples during storage.

**Data analysis.** Propagule populations for each of the three blocks were analyzed separately. The data were then combined into one composite block of 2,250 quadrats in a 15 × 150 quadrat grid. Thus, four sets of population data were used in most analyses, providing a variety of spatial patterns, which was particularly important in examining the robustness of various sampling strategies. For each of the four data sets, standard descriptive statistics (mean, variance) and the third and fourth moment statistics (skewness and kurtosis) were calculated (32).

Using FORTRAN computer programs developed by Gates and Ethridge (13), the Poisson, Neyman type A, and negative binomial discrete frequency distributions were fit to the four sets of data. These programs used a chi-square goodness-of-fit technique to assess the degree to which the data set was described by the particular distribution. The null hypothesis that the test distribution did not differ from the frequency count data was not rejected when the probability of a greater chi-square value equalled

or exceeded 0.05. Agreement with a Poisson distribution would imply a random spatial pattern (6), whereas agreement with the negative binomial or Neyman type A distributions would imply a nonrandom (aggregated) pattern (6). The Neyman type A distribution is less skewed than the negative binomial distribution (12).

Two indices of dispersion were calculated for each of the four data sets, the variance-to-mean ratio and Morisita's index of dispersion (21). The variance-to-mean ratio was tested for deviation from unity (12,33) with values significantly greater than one indicating aggregated spatial patterns. Morisita's index of dispersion was calculated from the following formula,

$$I_d = n((\Sigma(x^2) - \Sigma x)/((\Sigma x)^2 - \Sigma x)),$$

where $n$ is the number of quadrats and $x$ is the propagule population (21). The value of Morisita's index of dispersion was tested for deviation from unity, with a value of one indicating a random pattern (12,21,25). Values greater and less than one indicate an aggregated and uniform pattern, respectively (21). Morisita's index of clumping was calculated as the ratio of the index of dispersion for quadrat sizes $K$:$2K$ (21), where $K$ was a multiple of the primary quadrat size ($Q$) used for sampling. The index of clumping was calculated for $Q$, $2Q$, $4Q$, $8Q$, $16Q$, $32Q$, $64Q$, and $128Q$. Combined quadrats of sizes $2Q$, $4Q$, $16Q$, $64Q$, and $256Q$ were approximately square. Where combined quadrats were not square, combinations were done in both the $x$-direction (across rows) and the $y$-direction (down rows). For each combined quadrat, the propagule population of the original quadrat (size $Q$) most nearly in the center was used for the combined quadrat. To estimate aggregate (clump) size, Morisita's index of clumping is plotted as a dependent variable versus increasing quadrat size, $Q$ to $128Q$, as the independent variable. Peaks in this plot correspond to a situation where quadrat size is approximately equal to aggregate size (12,21). Multiple peaks indicate aggregation at several different levels.

Moran's I statistic of spatial autocorrelation was also calculated for each of the four data sets (8,20). This statistic was calculated from the following formula,

$$I = (n/W)\,((\Sigma_i\Sigma_j w_{ij} z_i z_j)/(\Sigma_i z_i^2)),$$

where $n$ is the number of quadrats, $w_{ij}$ is the weight assigned to the join between quadrats $i$ and $j$ (see below), $W$ is the sum of all weights, and $z_i$ and $z_j$ are the differences between the quadrat value and the mean, for quadrats $i$ and $j$, respectively. Positive values of I (positive autocorrelation) result when variate values in joined quadrats vary in the same direction from the mean, indicating that similar values tend to occur together. Negative I values (negative autocorrelation) result when variate values in joined quadrats vary in opposite directions from the mean. Initially, only quadrats with shared sides were considered joined. Joins between quadrats were weighted proportionally to the length of the shared side. To examine the behavior of the I statistic over distance (9,30,31), each quadrat within a block was compared with quadrats in 1-m-distance classes from 1–12 m distant. Quadrats were considered joined if the distance between their centers fell within the particular distance class.

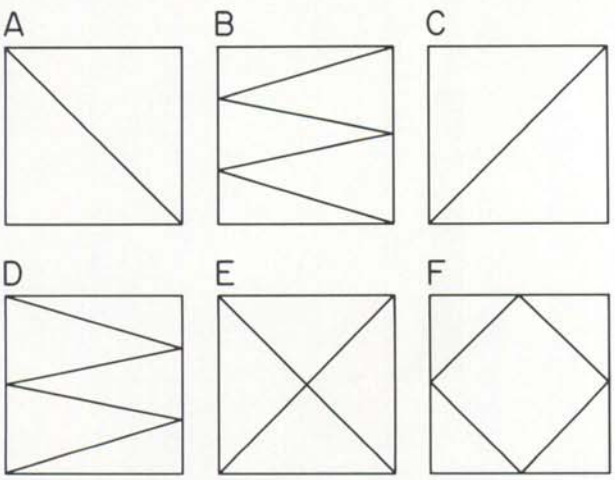


**Fig. 1.** Sampling paths for systematic site selection. **A,** Left diagonal. **B,** Right W. **C,** Right diagonal. **D,** left W. **E,** X. **F,** Diamond.

Two types of sampling strategies, systematic and probabilistic quadrat selection, were evaluated for their ability to accurately estimate the population mean. The evaluations were done with computer simulations, using the means from the four data sets as the populations parameters to be estimated by sampling. Systematic quadrat selection was examined using six standard systematic paths; right and left diagonal (RD, LD), right and left W (RW, LW), X, and diamond (D) (Fig. 1). For each path 5, 10, 15, 20, 25, or 30 quadrats were selected equally spaced along the path. The utility of probabilistic quadrat selection was evaluated using two survey sampling procedures (simple random sampling and cluster sampling) to estimate population means (26). For simple random sampling (SRS), 5, 10, 15, 20, 25, or 30 sample quadrats were selected. For cluster sampling, each data set was partitioned into nonoverlapping clusters where clustering was within rows. Clusters of three (CLU3) and five (CLU5) quadrats were used. For CLU3 simulations, 2, 4, 6, 8, or 10 clusters (6, 12, 18, 24, or 30 quadrats, respectively), were drawn, whereas two, three, four, five, or six clusters (10, 15, 20, 25, or 30 quadrats, respectively) were drawn for CLU5 simulations. Each SRS, CLU3, and CLU5 simulation, at each level of sampling intensity was repeated 30 times. All simulations for systematic and probabilistic quadrat selection were done with BASIC computer programs.

## RESULTS

The initial population in the bulk soil sample was 8.6 microsclerotia per gram ($n$ = 10, standard deviation = 2.81). Throughout the processing period, the bulk soil sample was assayed, with populations detected always less than one standard deviation from the mean. This indicates that the microsclerotial populations in the soil samples probably did not deteriorate appreciably during the several months required for processing the 2,250 samples.

Examination of the spatial pattern map for microsclerotia of *M. phaseolina* (Fig. 2) indicates a population increase from southwest to northeast across the field. Frequency distributions for each of the four data sets are illustrated in Figures 3 and 4. Microsclerotial population ranges were 1–19, 1–43, and 1–62 microsclerotia per gram for blocks 1, 2, and 3, respectively. These histograms show elongation at the high end of the ranges. This positive skewness was significantly greater than zero for all data sets (Table 1). Highly significant positive kurtosis for all blocks (Table 1) indicated leptokurtic distribution curves where more of the distribution density occurred near the mean and in the tails than would be expected for a normal distribution with the same mean and variance (32).

The four data sets were not adequately described by the negative binomial, Neyman type A, or Poisson discrete frequency distributions as indicated by highly significant chi-square values (Table 1).

The values of the two indices of dispersion (variance-to-mean ratio and Morisita's index) were significantly greater than one for all data sets, indicating aggregated (clustered) spatial patterns (Table 1). Morisita's index of clumping was used to estimate aggregate size for each of the four data sets (Table 2). In block 1, only one aggregate size was observed, between four and eight times the primary quadrat size ($4Q$, $8Q$), or 1.2–2.4 $m^2$. For the remaining data sets, two ranges of aggregate sizes were observed, a small aggregate size, generally between $2Q$ and $8Q$ (0.6–2.4 $m^2$), and a large aggregate size of at least $64Q$ (> 19.8 $m^2$). Elliott (12) noted that values of Morisita's index of dispersion approach the number of quadrats for patterns exhibiting maximum contagion. Thus, the comparison of index values based on differing numbers of quadrats may be flawed as these extreme conditions are

approached. During the construction of the index of clumping, the number of quadrats decreased as the size of combined quadrats increased (Table 2). However, the value of the dispersion index never exceeded 1.9, which is at least one order of magnitude smaller than the maximum possible values for combined quadrat sizes of $64Q$ or smaller. Thus, the conclusions presented concerning aggregates of size $64Q$ or smaller are probably still valid, whereas indications of larger aggregates should be interpreted with caution.

Moran's I statistic of spatial autocorrelation was calculated first for quadrats with shared sides. For all four data sets the I statistic was significantly greater than zero at $P = 0.001$ indicating positive autocorrelation (Table 1). Positive autocorrelation implies that like values tend to occur together. The I statistic was then calculated for quadrats increasingly distant from each other. The variation in the I statistic with distance is illustrated in a spatial corellogram (Fig. 5). The corellograms for blocks 2 and 3 were nearly identical, with significantly positive autocorrelation to a distance of 8 m. The value of I for block 1 was significantly greater than 0 for distances less than 4 m and for distances greater than 9 m.

The estimates of microsclerotia population of *M. phaseolina* based on the systematic selection of sampling sites are illustrated in Figure 6. Of the six paths tested, only the diamond (Fig. 6F) with 25 or 30 equally spaced sampling sites gave an estimate of the mean within 10% of the true population mean for all four data sets. The RD and RW paths gave good estimates for blocks 1 and 3, whereas the LD and LW paths gave poor mean estimates for all data sets. Because a priori knowledge of optimal placement for these paths is generally unavailable, the diagonal and W paths must be considered unsatisfactory. The estimates of the microsclerotial population of *M. phaseolina* based on probibilistic selection of sampling sites are illustrated in Figure 7. This strategy was unsatisfactory in providing a consistent estimate of the mean within 20% of the true population mean.

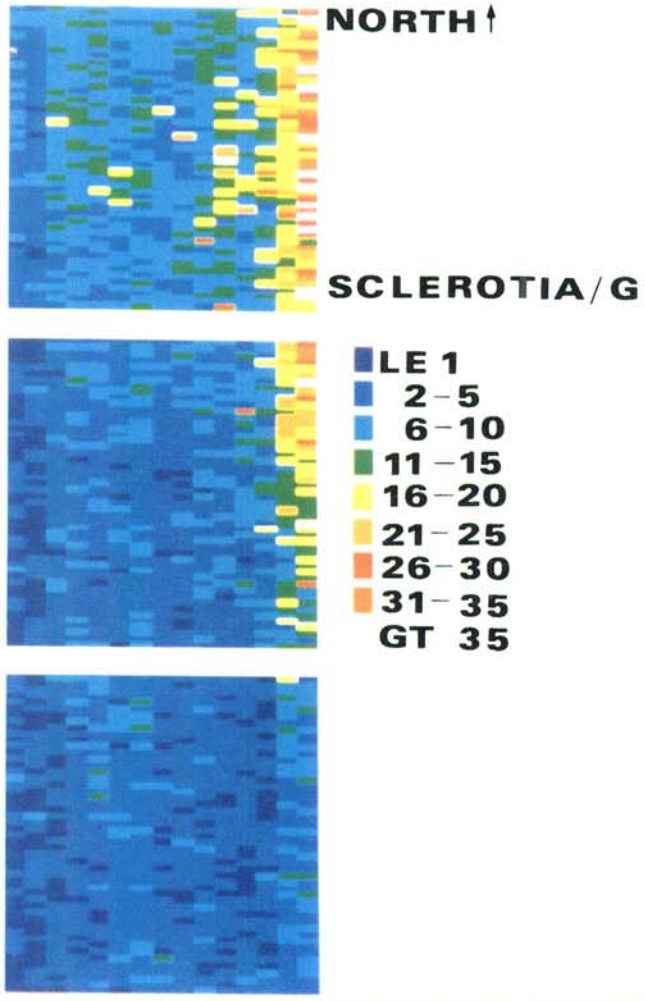


**Fig. 2.** Spatial pattern map of microsclerotia of *Macrophomina phaseolina* in a cultivated field at Marana, AZ. The blocks, from south to north are 1, 2, and 3.

## DISCUSSION

Studies of the propagule pattern of several soilborne fungi have revealed nonrandom patterns (1,34,35). Likewise, the pattern of microsclerotia of *M. phaseolina* in this study was found to be aggregated as measured by Morisita's index of dispersion. All four data sets showed significantly positive spatial autocorrelation as measured by Moran's I statistic (Table 1). The differences in spatial pattern among the three blocks, which are clear from Figure 2, were not adequately separated until Moran's I statistic was calculated for quadrats increasingly distant (Fig. 5) to examine the spatial lag. For block 1, the statistic became nonsignificant when quadrats 5–9 m distant were used but was significant at shorter and greater distances. For blocks 2 and 3, the I statistic was

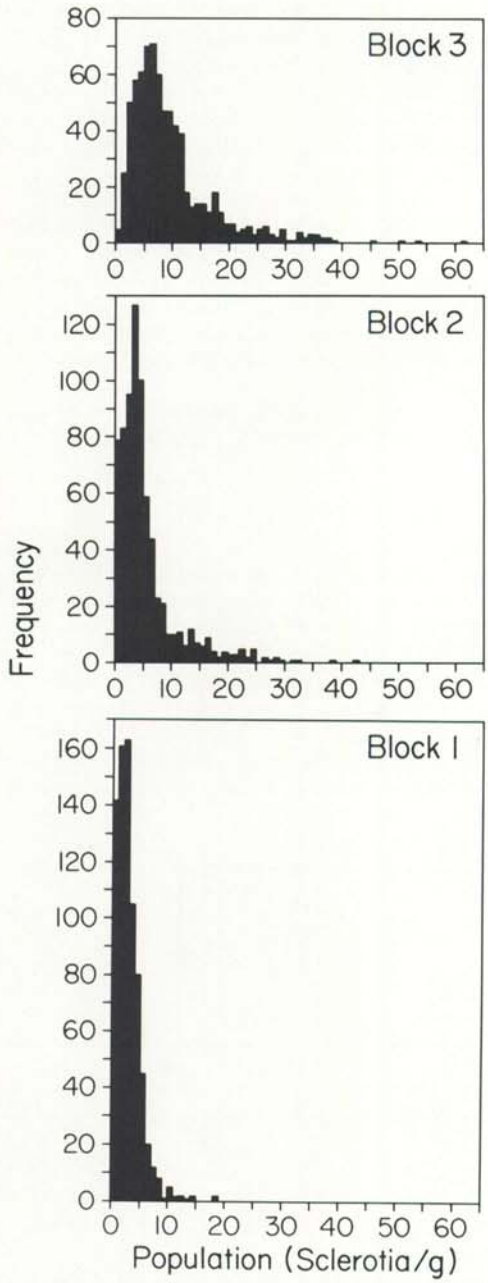


**Fig. 3.** Frequency distribution of microsclerotia of *Macrophomina phaseolina* for blocks 1, 2, and 3. For each block 750 quadrats were sampled.

significantly positive over a much larger distance. This relationship is referred to as high-order spatial lag (9,21) and is indicative of the presence of a gradient. Indeed, gradients of low populations in the west to high populations in the east can be seen for both blocks 2 and 3 (Fig. 2). Correlograms of this type should be considered a powerful tool for the comparison of inoculum density patterns. This characterization of the spatial pattern of microsclerotia of *M. phaseolina* is really just a single view of a dynamic system. Further work is in progress to characterize temporal changes in spatial patterns and to examine the implications for the development of charcoal rot in host populations.

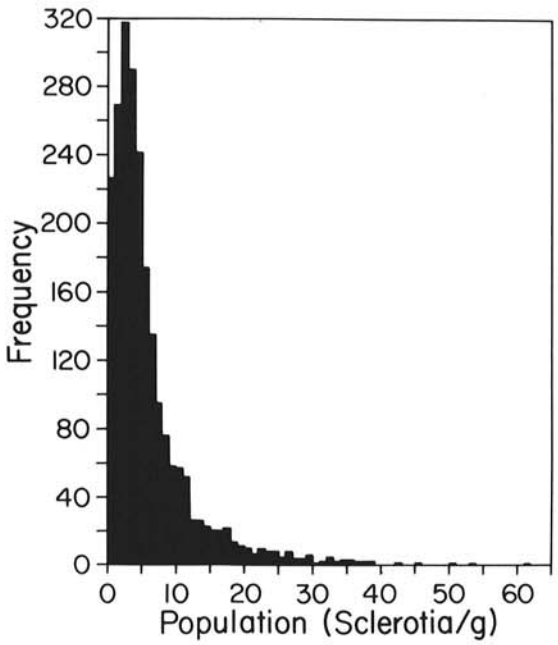


**Fig. 4.** Frequency distribution of microsclerotia of *Macrophomina phaseolina* for the composite block of 2,250 quadrats.

The choice of a sampling strategy is dependent on the type of information desired. If an estimate of the mean is all that is needed, collection of samples equally spaced along a systematic path through the field is sufficient. From results discussed in the present study, the diamond-shaped path, with a minimum of 25 equally spaced sampling sites along the path, gave the most consistent mean estimates for the four data sets (Fig. 6). Probabilistic site selection proved to be unsatisfactory because the microsclerotial populations were not randomly distributed. These results are in agreement with other studies. In a simulation study of nine

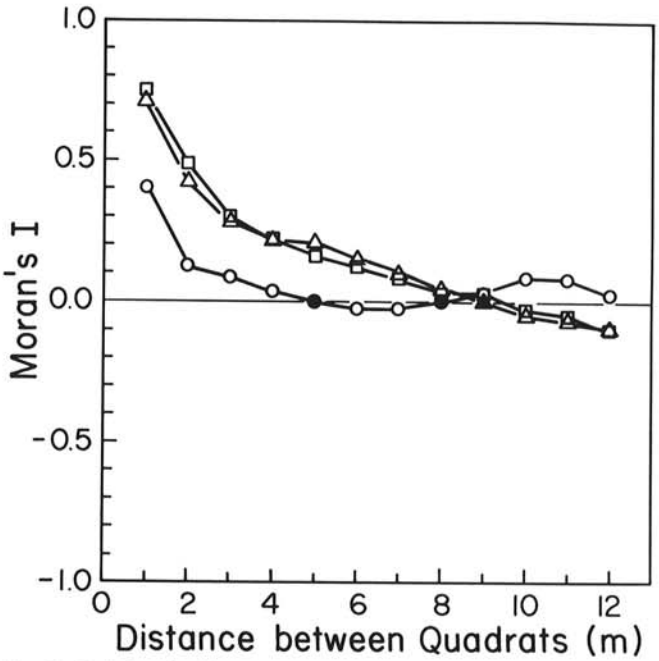


**Fig. 5.** Variation in Moran's I statistic of spatial autocorrelation with increasing distance between joined quadrats. Block 1 (o—o), block 2 (□—□), block 3 (Δ—Δ). Empty symbols indicate I significantly different than 0 at $P = 0.01$. Solid symbols indicate nonsignificant I values.

TABLE 1. Descriptive, dispersion, and spatial autocorrelation statistics for microsclerotial populations of *Macrophomina phaseolina*

| Block | Mean[a] | Skewness[b] | Kurtosis[c] | Variance-to-mean ratio[d] | Negative binomial[e] | Neyman type A[e] | Poisson[e] | Morisita's index[f] | Moran's I[g] |
|---|---|---|---|---|---|---|---|---|---|
| 1 | 3.4 | 1.90*** | 6.65*** | 1.52** | 105 | 118 | 155 | 1.15*** | 0.36*** |
| 2 | 5.9 | 2.53*** | 8.13*** | 5.24** | 234 | 576 | 2,512 | 1.71*** | 0.68*** |
| 3 | 10.3 | 2.15*** | 6.49*** | 5.88** | 128 | 325 | 4,161 | 1.47*** | 0.62*** |
| Composite | 6.5 | 2.69*** | 10.34*** | 6.19** | 508 | 2,247 | 29,400 | 1.79*** | 0.70*** |

[a] Sclerotia per gram of soil.
[b] A value of 0 indicates absence of skewness. *** = Skewness statistic significantly different from 0 at $P = 0.001$.
[c] A value of 0 indicates absence of kurtosis. *** = Kurtosis statistic significantly different from 0 at $P = 0.001$.
[d] ** = Ratio significantly greater than 1.0 at $P = 0.01$.
[e] For each discrete frequency distribution, the chi-square statistic is given. In all cases, the chi-square statistic was highly significant ($P < 0.01$) indicating that the frequency count data were not described by any of the frequency distributions.
[f] *** = Morisita's index of dispersion significantly greater than 1.0 at $P = 0.001$.
[g] *** = Moran's I statistic of spatial autocorrelation significantly greater than 0 at $P = 0.001$.

TABLE 2. Peaks in the plot of Morisita's index of clumping versus quadrat size[a]

| | Quadrat size[b] | | | | | | | | | | | | | | | |
|---|---|---|---|---|---|---|---|---|---|---|---|---|---|---|---|---|
| | Grouping across rows | | | | | | | | Grouping down rows | | | | | | | |
| Block | 1 | 2 | 4 | 8 | 16 | 32 | 64 | 128 | 1 | 2 | 4 | 8 | 16 | 32 | 64 | 128 |
| 1 | | | | * | | | | | | | * | | | | | |
| 2 | | * | | | | | * | | | * | | * | | | | * |
| 3 | | | * | | | | * | | | | | | * | | | * |
| (No. quadrats) | 750 | 375 | 180 | 84 | 42 | 24 | 12 | 6 | 750 | 375 | 180 | 90 | 42 | 21 | 12 | 8 |
| Composite | | | * | | | | | * | | | | * | | | | * |
| (No. quadrats) | 2,250 | 1,125 | 555 | 259 | 133 | 76 | 36 | 18 | 2,250 | 1,125 | 555 | 285 | 133 | 63 | 36 | 20 |

[a] To estimate aggregate (clump) size, Morisita's index of clumping is plotted as a dependent variable versus quadrat size (independent variable). Peaks in this plot (*) occur when quadrat size is approximately equal to aggregate size.
[b] Quadrat sizes are multiples of the primary quadrat size of 1.02 × 0.3 m.

systematic sampling paths for estimating microsclerotial populations of *Cylindrocladium cortalariae* (Loos) Bell and Sobers, Hau et al (15) found that only a diamond pattern and a pattern of three parallel diagonal paths gave mean estimates within 5% of the true mean, as determined by quadrat counts. The diamond path has the additional practical logistic advantage of returning the sampler to the point of origin, a nontrivial consideration when sampling large areas. In a simulation study of systematic paths through fields with varying spatial patterns, Lin et al (16) reported that with a random pattern, the number of samples was more important than the sampling pattern for precisely estimating a population mean. When simulated samples were taken from a clustered pattern, sampling pattern was critical with maximum dispersion of sampling sites giving the most precise estimates of the mean.

Mean estimation is quite useful where a known threshold level of a particular pathogen will influence the decision to plant. Otherwise, the estimation of a mean to characterize the population of a soilborne pathogen must be considered of limited utility, particularly where there is a great deal of variability in the population or where there is a gradient of host response to increasing pathogen populations. In this case, knowledge of population aggregation and aggregate size is highly desirable. When information of this type is needed, the use of quadrat count methods offers the additional opportunity to examine spatial patterns through autocorrelation and related analyses. The desirability of a large number of quadrats must be balanced against the cost of sample collection and processing. Frequently the cost of taking samples is much smaller than the cost of processing samples, making the processing of several hundred samples prohibitively expensive. Quantitative techniques are needed to rapidly assay soil for various phytopathogens so that more information than simply a mean and standard deviation may be routinely obtained. Lacking such rapid assay techniques, precision in population estimation may be increased by taking multiple soil samples in each quadrat,

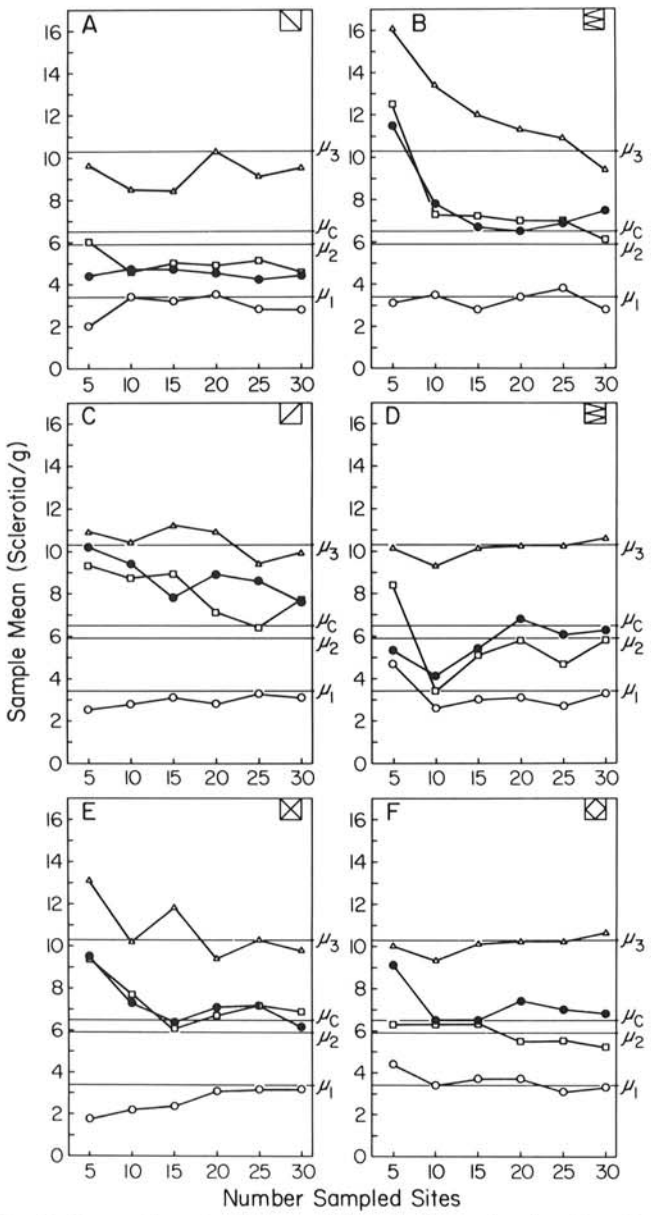


**Fig. 6.** Mean microsclerotial population of *Macrophomina phaseolina* estimated by systematic site selection. The simulated path used for site selection is indicated in the inset boxes. **A,** Left diagonal. **B,** Right W. **C,** Right diagonal. **D,** Left W. **E,** X. **F,** Diamond. The true population means are indicated by $\mu_1$, $\mu_2$, $\mu_3$, $\mu_c$ for blocks 1, 2, 3 and composite, respectively. Block 1 (o—o), block 2 (□—□), block 3 (Δ—Δ), composite block (•—•).

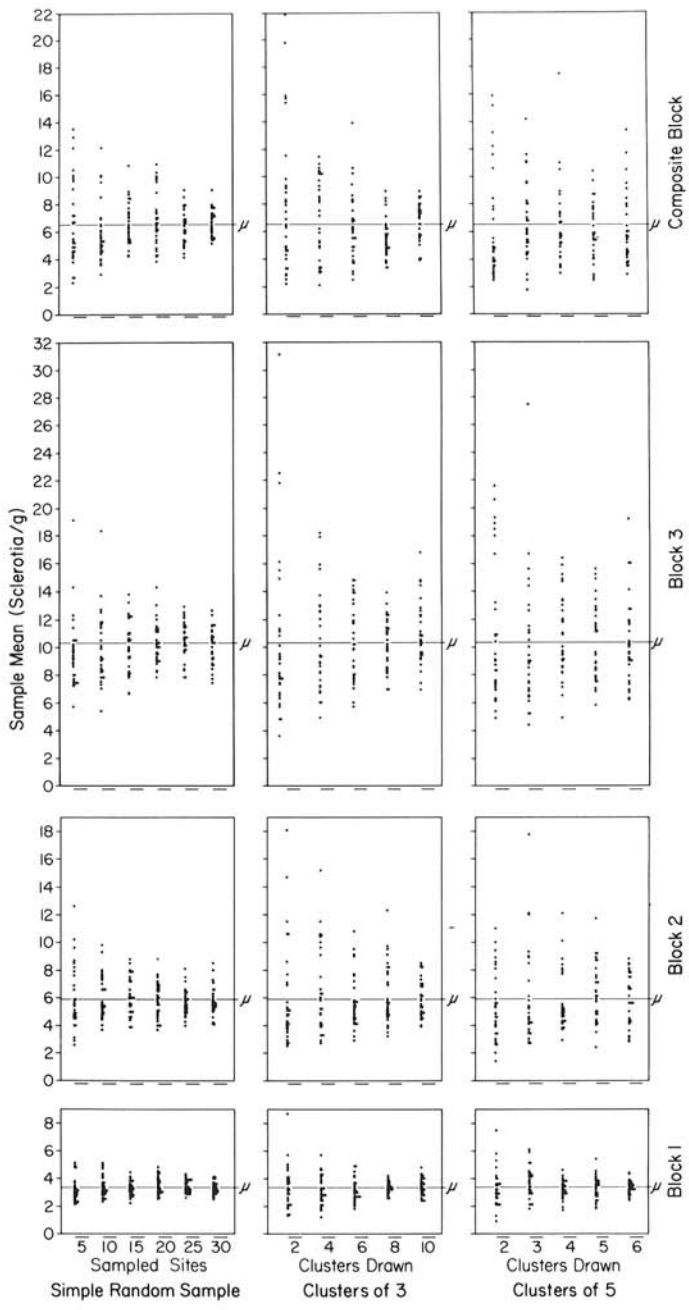


**Fig. 7.** Mean microsclerotial population of *Macrophomina phaseolina* estimated by probabilistic sample site selection. For each block, $\mu$ is the true population mean as calculated from all quadrat counts. Each plotted point represents a mean estimate from a single simulation. Thirty simulations were made for each sampling strategy at each level of sampling intensity.

and combining them. For Morisita's index of dispersion, the maximum quadrat size possible to still detect a nonrandom pattern was $8Q$, $64Q$, and $64Q$ for blocks 1, 2, and 3, respectively (where $Q$ is the primary quadrat size used for sampling). By comparing these results with the aggregate sizes for each block (Table 2), it is evident that the maximum quadrat size allowable to still detect nonrandomness is the same as the largest aggregate size. When quadrat size is larger than a particular aggregate size, then that aggregate size is nondetectable, and aggregation at that level is nondetectable. Thus, for block 1, using a quadrat size of $16Q$ would mean that aggregation would not be detected. Therefore, when selecting a quadrat size, it is important to note that all levels of aggregation smaller than the quadrat size chosen will be nondetectable.

It is clear that a gradient of sclerotial populations exists from low levels at the south end of the field to high levels at the north end (Fig. 2). In searching for an explanation for the observed pattern, it is important to consider the history of the field. A flood during early October 1983 irregularly deposited 20–25 cm of soil and debris over a large part of the experimental farm. During 1984, this material was incorporated into the field by disking. In early 1985, all fields on the farm were laser-levelled. Because the majority of the microsclerotia of *M. phaseolina* are found in the top 30 cm (4,19), the process of levelling could easily have caused the observed gradients of microsclerotia in the field. Thus, for pathogens, such as *M. phaseolina*, where infective propagules are concentrated near the soil surface, the impact of soil movement by routine cultural practices such as levelling, cultivation, etc., on the pattern of propagules and subsequent disease development merits further study.

## LITERATURE CITED


1. Adams, P. B. 1981. Forecasting onion white rot disease. Phytopathology 71:1178-1181.
2. Alby, T., Ferris, J. M., and Ferris, V. R. 1983. Dispersion and distribution of *Pratylenchus scribneri* and *Hoplolaimus galeatus* in soybean fields. J. Nematol. 15:418-426.
3. Benson, D. M., and Campbell, C. L. 1985. Spatial pattern of Phytophthora root rot and dieback of azalea in container-grown nursery stock. Plant Dis. 69:1049-1054.
4. Bruton, B. D., and Reuveni, R. 1985. Vertical distribution of microsclerotia of *Macrophomina phaseolina* under various soil types and host crops. Agric. Ecosyst. Environ. 12:165-169.
5. Campbell, C. L., and Nelson, L. A. 1986. Evaluation of an assay for quantifying populations of sclerotia of *Macrophomina phaseolina* from soil. Plant Dis. 70:645-647.
6. Campbell, C. L., and Noe, J. P. 1985. The spatial analysis of soilborne pathogens and root diseases. Annu. Rev. Phytopathol. 23:129-148.
7. Campbell, C. L., and Pennypacker, S. P. 1980. Distribution of hypocotyl rot caused in snapbean by *Rhizoctonia solani*. Phytopathology 70:521-525.
8. Cliff, A. D., and Ord, J. K. 1973. Spatial Autocorrelation. Pion Ltd. London. 178 pp.
9. Cliff, A. D., and Ord, J. K. 1981. Spatial Processes: Models and Applications. Pion Ltd. London. 266 pp.
10. Dhingra, O. D., and Sinclair, J. B. 1978. Biology and Pathology of *Macrophomina phaseolina*. Universidad Federal de Vicosa, Brasil. 166 pp.
11. Dillard, H. R., and Grogan, R. G. 1985. Relationship between sclerotial spatial pattern and density of *Sclerotinia minor* and the incidence of lettuce drop. Phytopathology 75:90-94.
12. Elliott, J. M. 1977. Some methods for the statistical analysis of samples of benthic invertebrates. Freshwater Biol. Assoc. Sci. Publ. 25. 144 pp.
13. Gates, C. E., and Ethridge, F. G. 1972. A generalized set of discrete frequency distributions with FORTRAN program. J. Int. Assoc. Math. Geol. 4:1-24.
14. Goodell, P. B., and Ferris, H. 1980. Sample optimization for five plant parasitic nematodes in an alfalfa field. J. Nematol. 13:304-313.
15. Hau, F. C., Campbell, C. L., and Beute, M. K. 1982. Inoculum distribution and sampling methods for *Cylindrocladium crotalariae* in a peanut field. Plant Dis. 66:568-571.
16. Lin, C. S., Poushinsky, G., and Mauer, M. 1979. An examination of five sampling methods under random and clustered disease distributions using simulation. Can. J. Plant Sci. 59:121-130.
17. Marois, J. J., and Adams, P. B. 1985. Frequency distribution analyses of lettuce drop caused by *Sclerotinia minor*. Phytopathology 75:957-961.
18. Martin, S. B., Campbell, C. L., and Lucas, L. T. 1983. Horizontal distribution and characterization of *Rhizoctonia* spp. in tall fescue turf. Phytopathology 73:1064-1068.
19. Mihail, J. D., and Alcorn, S. M. 1982. Quantitative recovery of *Macrophomina phaseolina* from soil. Plant Dis. 66:662-663.
20. Moran, P. A. P. 1950. Notes on continuous stochastic phenomena. Biometrika 37:17-23.
21. Morisita, M. 1959. Measuring the dispersion of individuals and analysis of the distributional patterns. Mem. Fac. Sci. Kyushu Univ. Ser. E 2:215-235.
22. Nicot, P. C., Rouse, D. I., and Yandell, B. S. 1984. Comparison of statistical methods for studying spatial patterns of soilborne plant pathogens in the field. Phytopathology 74:1399-1402.
23. Noe, J. P., and Campbell, C. L. 1985. Spatial pattern analysis of plant parasitic nematodes. J. Nematol. 17:86-93.
24. Punja, Z. K., Smith, V. L., Campbell, C. L., and Jenkins, S. F. 1985. Sampling and extraction procedures to estimate numbers, spatial pattern, and temporal distribution of sclerotia of *Sclerotium rolfsii* in soil. Plant Dis. 69:469-474.
25. Rohlf, F. J., and Sokal, R. R. 1981. Statistical Tables, 2nd ed. W. H. Freeman and Co., San Francisco, CA. 219 pp.
26. Scheaffer, R. L., Mendenhall, W., and Ott, L. 1979. Elementary Survey Sampling, 2nd ed. Duxbury Press, Belmont, CA. 278 pp.
27. Schuh, W., Frederiksen, R. A., and Jeger, M. J. 1986. Analysis of spatial patterns in sorghum downy mildew with Morisita's index of dispersion. Phytopathology 76:446-450.
28. Shew, B. B., Beute, M. K., and Campbell, C. L. 1984. Spatial pattern of southern stem rot caused by *Sclerotium rolfsii* in six North Carolina peanut fields. Phytopathology 74:730-735.
29. Smith, V. L., and Rowe, R. C. 1984. Characteristics and distribution of propagules of *Verticillium dahliae* in Ohio potato fields and assessment of two assay methods. Phytopathology 74:553-556.
30. Sokal, R. R., and Oden, L. 1978. Spatial autocorrelation in biology. 1. Methodology. Biol. J. Linn. Soc. 10:199-228.
31. Sokal, R. R., and Oden, L. 1978. Spatial autocorrelation in biology. 2. Some biological implications and four applications of evolutionary and ecological interest. Biol. J. Linn. Soc. 10:229-249.
32. Sokal, R. R., and Rohlf, F. J. 1981. Biometry, 2nd ed. W. H. Freeman and Co., San Francisco, CA. 859 pp.
33. Southwood, T. R. E. 1978. Ecological Methods. Chapman and Hall. London. 524 pp.
34. Stanghellini, M. E., von Bretzel, P., Kronland, W. C., and Jenkins, A. D. 1982. Inoculum densities of *Pythium aphanidermatum* in soils of irrigated sugar beet fields in Arizona. Phytopathology 72:1481-1485.
35. Taylor, J. D., Griffin, G. J., and Garren, K. H. 1981. Inoculum pattern, inoculum density-disease incidence relationships, and population fluctuations of *Cylindrocladium crotalariae* microsclerotia in peanut field soil. Phytopathology 71:1297-1302.
36. Thal, W. M., and Campbell, C. L. 1986. Spatial pattern analysis of disease severity data for alfalfa leaf spot caused primarily by *Leptosphaerulina briosiana*. Phytopathology 76:190-194.
37. Young, D. J., and Alcorn, S. M. 1982. Soil populations of *Macrophomina phaseolina* in Arizona. (Abstr.) Phytopathology 72:993.
38. Young, D. J., and Alcorn, S. M. 1984. Latent infection of *Euphorbia lathyris* and weeds by *Macrophomina phaseolina* and propagule populations in Arizona field soil. Plant Dis. 68:587-589.